

The initial distribution and evolution of globular cluster systems

H. Baumgardt

Astronomisches Rechen-Institut Heidelberg, Mönchhofstraße 12-14, D-69120 Heidelberg, Germany
e-mail: holger@ari.uni-heidelberg.de

Received 17 April 1997; accepted 13 August 1997

Abstract. This work considers the evolution of globular cluster systems in galaxies. Here globular cluster systems start with power-law mass functions $\phi \sim M^{-\alpha}$ with slopes around 2.0, similar to what has been observed for the young luminous clusters seen in merging and interacting galaxies. We then follow the orbits of the clusters through their parent galaxy, allowing various destruction mechanisms to dissolve them. In comparing the surviving distribution to the observed one, we show that our model can reproduce several aspects of present day globular cluster systems.

This method is employed to the globular clusters of the Milky Way and M87. In the case of the Milky Way we obtain luminosity distributions, which depend on the galactocentric distance in a way similar to what is observed. We also observe a change in the velocity distribution of the globular cluster system, which predicts a different kinematical state of the surviving halo clusters compared to the halo stars. The final luminosity function of the globular cluster system in M87 can differ from the one found for the Milky Way clusters, which casts doubt on the use of globular cluster luminosity functions to measure distances. We also discuss some implications of our results for the dynamical history of M87.

Key words: Galaxy: globular clusters: general – Galaxies: star clusters – Galaxies: individual: M87

1. Introduction

Globular clusters represent a part of the oldest stellar sub-systems of galaxies, and understanding the details of their formation and evolution allows valuable insights in the early history of galaxies. One of the most remarkable features of globular cluster systems is their luminosity distribution. The globular clusters of the Milky Way for exam-

ple have typical masses in the range of $10^5 - 10^6 M_{\odot}$ and a Gaussian luminosity distribution, similar to the globular clusters in other galaxies (Harris 1991). Globular clusters are in striking contrast to star clusters which are currently being formed, such as the galactic open clusters and the young luminous clusters (YLCs). The open clusters of the Milky Way, for instance, have a power-law distribution of masses with slope $\alpha \approx 2$ (Battinelli et al. 1994) and typical masses in the range $10^2 - 10^3 M_{\odot}$.

YLCs are found in a wide variety of environments, ranging from the Magellanic Clouds up to interacting and merging galaxies. Since it is likely to find YLCs in interacting galaxies and since these objects are also found in galaxies having circumnuclear rings it seems they are common in all galaxies experiencing enhanced star formation. YLCs have a power-law distribution of luminosities with a slope resembling that of the galactic open clusters, so it seems they are closely related to them. In contrast Ho & Filippenko (1996a,b) have recently shown that the masses of the most massive objects reach beyond $10^5 M_{\odot}$, which is far more massive than what has been observed for open clusters. Given the masses and spatial extension (Maoz et al. 1996), YLCs look like young counterparts of the galactic globular clusters, and the question arises whether the galactic globular cluster system has started with a similar distribution of masses.

In this paper we examine the hypothesis if globular cluster systems start with power-law mass functions. We first distribute a number of globular clusters (typically 100000) according to a stable initial condition. In the case of the Milky Way for example, the cluster system has initially a spatial and velocity distribution typical for the stellar halo. We then follow the orbits of the clusters through their parent galaxy with a leap-frog algorithm, allowing various destruction processes to work on them. If the mass of a cluster falls below $10^3 M_{\odot}$, it sinks toward the galactic center or the ratio of the half-mass radius to the tidal radius exceeds a critical value, it is expelled from the calculation. After a Hubble-time the surviving

distribution is compared to the observed one under various aspects. Similar calculations are presented for clusters in the giant elliptical galaxy M87.

This paper is organised as follows: In Sect. 2 we discuss the destruction processes. The initial distribution of the clusters and related problems will be discussed in Sect. 3 and in the following section we will present the results. Finally we draw some conclusions on the evolution of systems of star clusters.

2. The destruction processes

2.1. Internal dissolution and the galactic tidal field

In this section we will discuss the evaporation of star clusters. We use a simple parametrization for that purpose. We do not include stellar evolution, since we expect that this process is only important in the early stage of cluster evolution. Therefore our considerations are valid for a time after all massive stars have reached their endstates, which is roughly 100 Myr after cluster formation. We also do not consider any change in the structural parameters of the clusters.

2.1.1. Isolated clusters

The most important destruction process for star clusters is mass loss through mutual encounters of the cluster stars. Stars gain energy in such encounters, which will cause their velocities to change in magnitude and direction and some stars, which get more than the escape energy will leave the cluster. Following Spitzer & Hart (1971) the time it will take for a typical cluster star to change its velocity completely is given by

$$t_{rh} = 0.138 \frac{\sqrt{M_c} r_h^{3/2}}{\langle m \rangle \sqrt{G} \ln(0.4N)}. \quad (1)$$

Here M_c is the mass of the cluster, r_h its half-mass radius, G is the gravitational constant, $\langle m \rangle$ is the mean mass of the cluster stars and $N = M_c / \langle m \rangle$ is the number of stars in the cluster. For our clusters we adopt a mass function according to Kroupa et al. (1993), with upper limit $m_u = 1.2 M_\odot$ and lower limit $m_l = 0.15 M_\odot$. We derive a mean mass of $\langle m \rangle = 0.41 M_\odot$ this way. The timescale (1) is usually referred to as the half-mass relaxation time. Since it is the time in which a typical cluster star changes its velocity, it is naturally to assume that the mass-loss of the whole cluster happens on a comparable timescale. Following Hénon (1961), we therefore adopt for the mass loss:

$$dM_c = -\xi_0 M_c \frac{dt}{t_{rh}}. \quad (2)$$

For our clusters we assume a steady mass-loss rate and take the initial relaxation time rather than the actual one, which would speed up the mass-loss. The constant ξ_0 is

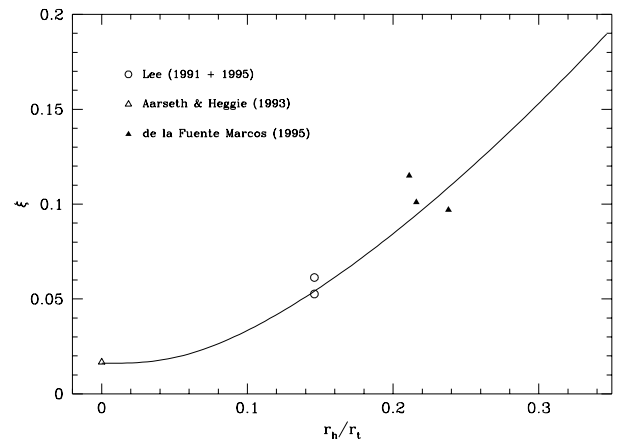


Fig. 1. Run of $\xi = \xi_0 \sqrt{1 + (\alpha \frac{r_h}{r_t})^3}$ with r_h/r_t .

best determined from simulations of star clusters with a realistic mass spectrum. Aarseth & Heggie (1993) for example performed a N-body calculation with 5820 single stars and 180 binaries. They derived a mass-loss which corresponds to $\xi_0 \approx 0.016$ in our notation. We adopt this value as the mass-loss of an isolated cluster.

2.1.2. The presence of a tidal field

An external tidal field greatly enhances the mass-loss rate. One observes that the lifetimes of tidally limited clusters become independent of their half-mass radius and a function of the tidal radius alone (see for example McMillan & Hut 1994). Following Wielen (1988), we therefore adopt for the mass-loss:

$$dM_c = -\xi_0 \sqrt{1 + (\alpha \frac{r_h}{r_t})^3} M_c \frac{dt}{t_{rh}}. \quad (3)$$

This formula has the desired property. It also approaches (2) in the limit $r_t \rightarrow \infty$, as it should be. The parameter α is determined from fitting our formula to the results of Lee et al. (1991), Lee & Goodman (1995) and de la Fuente Marcos (1995, Models XXII - XXIV) (see Fig. 1). In this way, we obtain the value $\alpha = 14.9$. Our mass-loss rates are somewhat higher than the ones found by Wielen (1988). For a tidally limited star cluster of mass $M_c = 1000 M_\odot$ our formula predicts a lifetime, which is about a factor of two shorter than his prediction. To check the dependance of our results on that point we make simulations with all mass-loss rates halved.

Since every star cluster moves on a more or less eccentric orbit it is exposed to a varying tidal field. To discover the radius which determines the evolution of such a cluster, we performed N-body-simulations of three star clusters. All clusters were composed out of 1000 equal mass stars with mass $m_* = 1 M_\odot$ and had the same half-mass

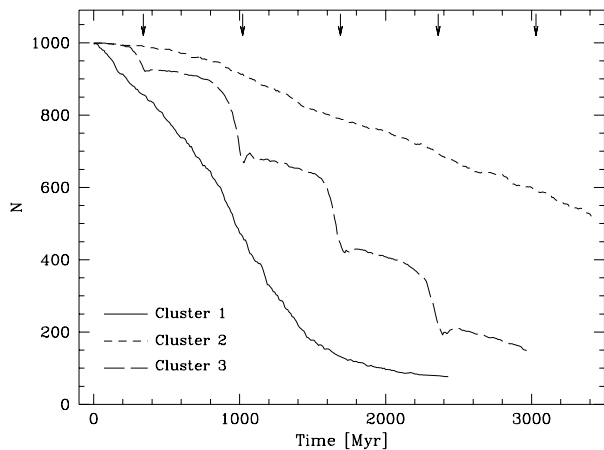


Fig. 2. Number of bound stars as a function of time for the 3 star clusters. The arrows at the upper side indicate the perigalactic passages of cluster 3.

radius and density profile. Cluster 1 was moving in a circular orbit with radius $R_{GC} = 8.5$ kpc and speed $v_{circ} = 220$ km/sec around a galaxy which was modeled as a point mass. Cluster 2 was orbiting in a circular orbit with radius $R_{GC} = 25.5$ kpc. Cluster 3 had an eccentric orbit between the two galactocentric distances $R_{Peri} = 8.5$ and $R_{Apo} = 25.5$ kpc. For all clusters the tidal radius was calculated according to

$$r_t = \left(\frac{M_c}{3 M_G} \right)^{1/3} R_{GC} \quad (4)$$

with M_G being the mass of the galaxy and R_{GC} the instantaneous distance of the cluster to the center of the galaxy. Stars with a distance $r > r_t$ from the center of the cluster were counted as escapers. The number of stars left in the different clusters as a function of time is shown in Fig. 2. As one can see, cluster 1 loses its stars with an approximately constant rate until only 200 stars are left. Afterwards the mass-loss is strongly reduced. Neglecting this final stage and defining the dissolution time as the time when less than 200 stars are left, one obtains the dissolution time of cluster 1 to be 1400 Myr. Extrapolating the mass-loss of cluster 2, one would expect that the number of bound stars of this cluster will drop below 200 around $T = 6000$ Myr. The dissolution of cluster 3 proceeds in a very irregular way. A lot of stars are stripped away during the perigalactic passages and the mass-loss is lower afterwards. At $T = 2400$ Myr the number of bound stars drops below 200. Although the dissolution time of cluster 3 is higher than that of cluster 1, both are much smaller than that of cluster 2. So it seems, that the tidal radius at the innermost point of an eccentric orbit determines the dissolution of a star cluster. In the simulations

we therefore take the tidal radius in equation (3) at the innermost point of the cluster orbit.

2.2. Dynamical friction

If a cluster moves through a sea of background particles (usually stars) it will accelerate them. The increase in energy of the background particles is taken from the orbital energy of the cluster. This process is known as dynamical friction. It will cause the cluster to sink toward the galactic center. Following Binney & Tremaine (1987) the loss of speed of the cluster is given by:

$$\frac{dv_c}{dt} = -\frac{4\pi \ln(\Lambda) G^2 \rho M_c}{v_c^3} \left(\operatorname{erf}(X) - \frac{2X}{\sqrt{\pi}} e^{-X^2} \right) v_c \quad (5)$$

with

$$X = \frac{|v_c|}{\sqrt{2}\sigma}. \quad (6)$$

Here v_c is the speed of the cluster, ρ is the density of the background objects and σ is their velocity dispersion which was assumed to be 210 km/sec. We found that dynamical friction is only important for high mass clusters ($M_c \gtrsim 10^6 M_\odot$) close to the galactic center ($R \lesssim 2$ kpc).

2.3. Disk shocking

The disk possesses a varying tidal field to the clusters which will cause a speed up of the stars each time a cluster passes through its plane. It was impossible to model this effect, because most papers found in the literature consider only the energy increase of the whole cluster. Since a large part of this energy will be carried away by escapers the fate of a cluster after a passage through the galactic disk remains uncertain. Disk shocking may be an important destruction mechanism for some clusters (Weinberg 1994). But it seems that it is only a minor effect for the destruction of the whole cluster system (Ostriker et al. 1972, see also Gnedin & Ostriker 1997).

3. Initial condition and related problems

3.1. The distribution of cluster masses

The distribution of masses is assumed to be a power-law: $\phi(M) \sim M^{-\alpha}$. The observed slopes of YLCs range from about 1.8 in the case of the galaxies with the greatest number of YLCs (and hence the best measurable value) NGC 4038/39 (Whitmore & Schweizer 1995) to slopes around 2.0. Calculations were done with these two values for the slope α . The lower and upper limit of the cluster masses were chosen to be $10^3 M_\odot$ and $3 \cdot 10^6 M_\odot$ respectively. Adding clusters with masses lower than $10^3 M_\odot$ would not affect the results, since such clusters evaporate completely over a Hubble-time. To transform the final distribution of masses into one of luminosities a mass-to-light ratio $(M/L)_V = 2.0$ was used.

3.2. The initial distribution of half-mass radii

In our simulations the half-mass radii of the clusters were initially distributed between two values, which are a function of their mass M_c and their galactocentric distance R_{GC} . The clusters were distributed uniformly between them or their logarithm.

The lower bound of the half-mass radii of the clusters was chosen in a way that the clusters do not become too dense compared to the present day clusters. Looking at the distribution of the galactic globular clusters in the mass-half-light-radius plane (Fig. 3), one can see that there exist no clusters for which the 'density' $\rho_h = M_c/r_{hp}^3$ exceeds a value of $10^5 M_\odot/\text{pc}^3$. Clusters with masses around $10^6 M_\odot$ and radii of several parsecs have relaxation times of the order of $3 \cdot 10^9$ yrs. Since it takes several half-mass relaxation times for core collapse, and since the half-mass radius of a cluster only expands in the post-collapse phase, one would expect the half-mass radii of these clusters not to be significantly affected by internal relaxation. The absence of clusters in this region must hence reflect the initial conditions. The lower limit of r_{hp} was chosen to be 0.3 pc since one observes no clusters (globular or open (Lyngå 1987)) with sizes smaller than that. We note that adding smaller clusters will not affect the final distribution, since these clusters have such small relaxation times that they dissolve completely during the calculation.

In order to derive the spatial half-mass radii from the projected half-light radii, we first assumed a constant mass-luminosity ratio of the cluster stars independent of distance to the cluster center. Second a ratio of $r_h/r_{hp} = 1.37$ was assumed. This is exactly true for King models (King 1966) with $W_0 = 7.0$, the mean concentration of the galactic globular clusters. Other King models with realistic concentrations ($2 \leq W_0 \leq 11$) differ by no more than 0.1 from this ratio.

The upper bound for the half-mass radii can be derived in two ways. Looking at the clusters relatively close to the galactic center ($R_{GC} < 10.0$ kpc) one sees that there are no clusters with ρ_h lower than $10^3 M_\odot/\text{pc}^3$. The outer clusters ($R_{GC} > 10.0$ kpc) violate this relation, but one has to bear in mind that the tidal radii of outer clusters are so large that clusters with half-mass radii of a few pc are nearly isolated. Since it is a well established fact known from many N-body-Simulations, that isolated clusters expand in the post-collapse phase (see for example Giersz & Heggie 1994, Giersz & Heggie 1996), it is possible that clusters with $\rho < 10^3 M_\odot/\text{pc}^3$ were much smaller at the time of their formation. So an upper limit for the half-mass radii can be derived by requiring

$$\rho_h = \frac{M_c}{r_{hp}^3} > 10^3 \frac{M_\odot}{\text{pc}^3}. \quad (7)$$

We also made a calculation requiring $\rho_h > 10^2 M_\odot/\text{pc}^3$ to check the dependance of our results on this assumption.

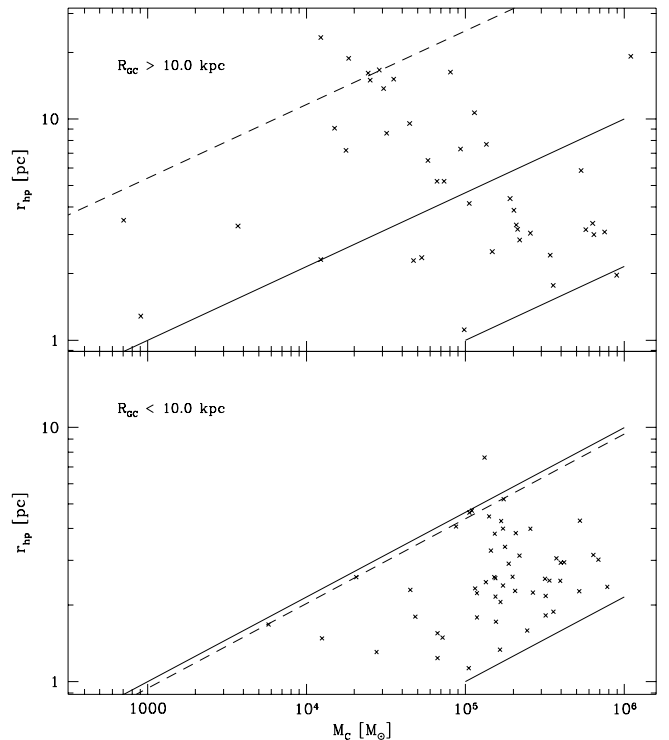


Fig. 3. Plot of cluster half-light radius r_{hp} , containing half of the light in projection vs. cluster mass M_c . The solid lines correspond to densities of $\rho_h = 10^3$ and $10^5 M_\odot/\text{pc}^3$ respectively. The dashed lines are the tidal radii for clusters located at 10 kpc (upper panel) and 1 kpc (lower panel) multiplied by x_{crit} . We note, that hardly any clusters are found in the region above these lines.

Another way to derive an upper limit is to look at the tidal radius of the clusters. The half-mass radius of a cluster must be sufficiently smaller than its tidal radius. Otherwise the tidal field of the Galaxy would quickly remove a large fraction of the stars, which would cause the tidal radius to shrink. Again a large fraction of the remainder stars would escape. If the ratio of the half-mass radius to the tidal radius exceeds a critical value x_{crit} , this process would result in a cluster disruption on a dynamical timescale. x_{crit} was chosen to be 0.3, calculations were also done with $x_{crit} = 0.5$ without affecting the results significantly. So a second condition for the upper limit is

$$x_{crit} = \frac{r_h}{r_t} \leq 0.3. \quad (8)$$

In setting up the initial distribution the more stringent of the above two conditions was used. Since we do not include stellar evolution, our starting value for the half-mass radius should be considered as the radius of the equilibrium configuration after the massive stars have gone supernova. Our upper limit is in good agreement with the values found by Goodwin (1997) in his detailed calculations of cluster formation.

In the simulations, clusters are removed, when the ratio of their half-mass radius to the tidal radius taken at their actual position in the Galaxy exceeds x_{crit} . This is supported by the fact that one sees (almost) no clusters above the dashed lines in Fig. 3.

We proceeded in the following way: we first choose the mass and the galactocentric distance of each cluster, then the individual upper and lower limits of the half-mass radii were calculated, and finally a radius to each cluster was assigned. We assume that the formation of a cluster out of its parent molecular cloud takes place on a short timescale compared to the orbital time of the cluster. Therefore we took the initial galactocentric distance to calculate the cluster radius.

3.3. The model for the Milky Way

Our model for the Milky Way consists of four parts: the central black hole, the bulge, the disk and the dark corona. Following Krabbe et al. (1995) the center of our galaxy harbours a black hole of mass $3 \cdot 10^6 M_{\odot}$. The bulge is taken to be a Plummer sphere with total mass $M_B = 1.406 \cdot 10^{10} M_{\odot}$ and core-radius $b = 0.387$ kpc.

The disk is usually assumed to follow a double-exponential density law. For the sake of simplicity we replaced the disk by a spherical component, which has the same amount of material inside a sphere of radius r like the disk inside a cylinder of radius r . So our new 'disk' follows the density law

$$\rho \sim \frac{1}{r} e^{-r/r_0} \quad (9)$$

with radial scale length $r_0 = 3.5$ kpc. We did this simplification because all components are spherical afterwards and it is much simpler to find stable initial conditions for spherical systems than for axisymmetric ones. The total mass of the disk is $8.56 \cdot 10^{10} M_{\odot}$.

The dark corona finally is assumed to be a softened isothermal sphere

$$\rho = \frac{\rho_0}{1 + \frac{r^2}{a^2}} \quad (10)$$

with central density $\rho_0 = 3 \cdot 10^7 M_{\odot}/\text{kpc}^3$ and softening length $a = 5$ kpc.

3.4. The distribution of the clusters in the Milky Way

The globular cluster system of the Galaxy can be divided into two parts (Zinn 1985, Djorgovski & Meylan 1994). Metal-poor clusters ($[\text{Fe}/\text{H}] < -1.0$) are generally thought to be connected to the stellar halo on the basis of their similar metallicities and spatial distribution. Metal-rich clusters ($[\text{Fe}/\text{H}] > -1.0$) on the other hand are located much closer to the Galactic plane and are thought to be connected with the thick disk (Armandroff 1989) or bulge

(Minetti 1995). In this paper we want to draw our attention to the evolution of the halo globular cluster system, so for the comparison of our predictions with the observations the metal-rich clusters are omitted.

The YLCs do not arise alone. Instead one always observes the contemporary formation of field stars and star clusters. One also observes that the YLCs and the field stars have the same projected distribution. This is true for galaxies having starforming rings and could also be shown for two galaxies which are thought to be the remnants of merging processes: NGC 7252 (Whitmore & Schweizer 1993) and NGC 3921 (Schweizer et al. 1996). So it is reasonable to assume that the globular cluster system has initially the same spatial distribution as the stellar halo.

The density-profile of the stellar halo is normally fitted by a power-law $\rho \sim r^{-\gamma}$. The steepness of the power-law is found to be $\gamma = 3.5$ in the solar neighbourhood (Zinn 1985, Preston et al. 1991) with the possibility of becoming steeper in the outer parts. This is similar to the halo of M31, where Pritchett & van den Bergh (1994) found that the density falloff becomes progressively steeper ranging from $\rho \sim R^{-2.5}$ at $R < 2$ kpc to $\rho \sim R^{-5.0}$ between 10 and 20 kpc. We adopted a density law of the form

$$\rho \sim \frac{1}{1 + \left(\frac{r}{a}\right)^{\gamma}} \quad (11)$$

The softening length a was chosen to be $a = 0.5$ kpc and we made calculations with $\gamma = 3.5, 4.0$ and 4.5 .

3.5. The initial velocity distribution

For the globular cluster system we assumed a distribution function of the form

$$f(E, L) = f(E) \cdot L^{-2\beta} \quad (12)$$

with E being the orbital energy of a cluster, L its angular momentum and β the ratio of the tangential to the radial velocity dispersion:

$$\beta(r) = 1 - \frac{\sigma_t^2}{\sigma_r^2} \quad (13)$$

with $\sigma_t^2 = \frac{1}{2}(\sigma_{\phi}^2 + \sigma_{\theta}^2)$. This distribution function leads to a system with constant anisotropy β independent of r and has the advantage that $f(E)$ can be calculated once the galactic potential and the density profile of the cluster system are chosen. We note that in the absence of destruction processes our cluster systems are in stable dynamical equilibrium.

The system of halo stars is generally thought to be radially anisotropic. Morrison et al. (1990) give the velocity ellipsoid of a kinematically unbiased halo sample from which metal-poor thick disk stars have been removed as $(\sigma_r, \sigma_{\phi}, \sigma_{\theta}) = (133 \pm 8, 98 \pm 13, 94 \pm 6) \text{ km s}^{-1}$. One obtains $\beta = 0.48$ for these stars. Similar values of β can be derived from the velocity ellipsoids of Sommer-Larsen et

al. (1994) ($\beta \approx 0.63$ in the solar neighborhood), and Beers & Sommer-Larsen (1995) ($\beta = 0.57$). Most of our calculations have $\beta = 0.5$. In addition, we also tried $\beta = -\infty$ and 0.7. One has to bear in mind that the velocity ellipsoid of the outer parts of the halo could be more tangentially anisotropic (Sommer-Larsen et al. 1994).

3.6. The age of the cluster system

The ages of globular clusters can be derived by comparing an aspect of their color-magnitude diagrams (CMDs) to theoretical models. For example Chaboyer et al. (1996) used the absolute magnitude of the main-sequence turnoff to derive ages for clusters with well established CMDs. They found that the mean of the cluster ages is about 16.0 Gyr with a total dispersion of 5 Gyr. They find no strong evidence for an age - galactocentric distance relationship. The derived ages are consistent with the assumption that star formation began throughout the halo at the same time. These results are confirmed by Richer et al. (1996), who found no significant correlation between mean cluster age and galactocentric distance and only a slight age difference, if any at all, between metal-poor and metal-rich halo clusters. We therefore adopt an age of $T = 16$ Gyr for all clusters.

3.7. The model for M87

We first have to choose a distance to M87 before we can determine the other parameters. New distances to spirals in the direction of the Virgo cluster derived from HST observations of cepheids yield values around $D = 16.0$ Mpc (Ferrarese et al. 1996, Saha et al. 1996ab). The only exception is NGC 4639 with a distance estimate of $D = 25.1$ Mpc (Sandage et al. 1996). Since M87 is the central galaxy in this cluster, it should be between the other galaxies. In the first case we take the mean of all measurements and set the distance to $D = 18$ Mpc. Unless otherwise stated all statements belong to this distance. In the second case we omit the far galaxy as being behind the Virgo cluster and adopt a distance $D = 16$ Mpc to M87.

For the calculation of the potential we assume M87 to be composed out of three components. The first is the central black hole. Its mass is taken to be $3.4 \cdot 10^9 M_{\odot}$ (Ford et al. 1994, Travis 1994). The second component is made up of the visible stars. They are assumed to follow a de Vaucouleur profile with effective radius $R_e = 96.0''$ (Surma et al. 1990, de Vaucouleur & Nieto 1978). Our globular cluster system has initially the same distribution. The dark matter is the third component, which we take to be a softened isothermal sphere. The mass of the latter two components can be found through simultaneous fitting the velocity dispersion of the stars in the inner part of M87 (as observed by Sargent et al. 1978) and from the ROSAT observations of the X-ray profile of the hot gas surrounding

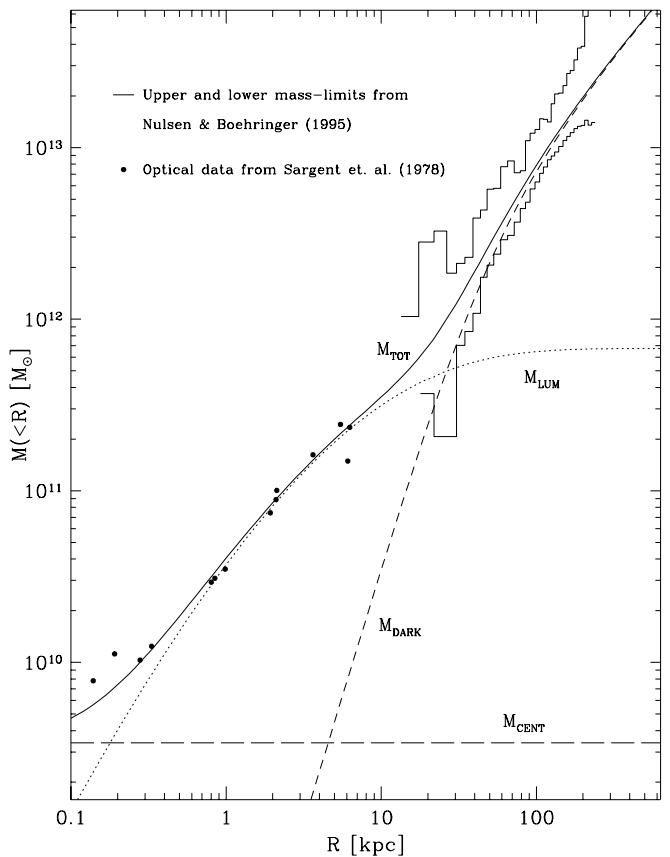


Fig. 4. Mass enclosed inside a sphere of radius R around the center of M87, assuming a distance $D = 18$ Mpc.

M87 (Nulsen & Böhringer 1995) (Fig. 4.). The total mass in the form of stars is found to be $6.7 \cdot 10^{11} M_{\odot}$.

The velocity anisotropy is known for stars in the inner parts of M87. Van der Marel (1994) finds, that a value of $\beta = 0.478$ is the best fit to the velocity profile inside a radius $r < 25$ arcsec. Consequently we adopt a value of $\beta = 0.5$ throughout M87.

While it seems to be appropriate to assume the same age for all Milky Way clusters, this is no longer true for M87. For example Elson & Santiago (1996; henceforth ES) find a bimodal color distribution in their globular cluster sample. They find that the blue clusters have colors comparable to the Milky Way clusters, while the red clusters are absent in our galaxy. ES note that if elliptical galaxies form from the merger of spiral galaxies, then the blue clusters may represent clusters native to the galaxies which merged, while the red clusters may have formed during the merger. We therefore assume an age of 16 Gyr for the blue clusters, an age of 10 Gyr for the red clusters and make our calculations with the mean age $T = 13$ Gyr.

4. Results

4.1. Results for the Milky Way globular cluster system

We performed calculations with different values of the slope of the initial power-law index α , the anisotropy parameter β and the radial steepness of the cluster density distribution. Since nothing is known about the half-mass radii of the globular clusters at the point of their formation, we tried different initial distributions over half-mass radius. In case 1 the probability for a cluster to have a radius between $\log(r_{hp})$ and $\log(r_{hp}) + \log(dr)$ is constant for $\log(r_{low}) \leq \log(r_{hp}) \leq \log(r_{up})$ and 0 elsewhere. In case 2 the probability is constant between $r_{low} \leq r_{hp} \leq r_{up}$ and 0 elsewhere. This represents a case biased to high radii. The parameters of the different runs are summarized in table 1.

We divide our final cluster system into two parts: the inner clusters that have $R_{GC} < 10$ kpc and the outer clusters with $R_{GC} > 10$ kpc at the end of the calculation. This division is valid for the rest of this section. In order to compare our results to the Milky Way clusters we use the recent compilation of cluster data by Harris (1996). To obtain a pure halo sample, we expelled all clusters with $[\text{Fe}/\text{H}] > -1$, or if the metallicity of a cluster is not known, we removed clusters with $R_{GC} < 15.0$ kpc from this dataset. We are left with a total number of 98 halo clusters, with which we compare our results.

Table 1. Initial parameters of the performed runs

Run	α	β	γ	ρ_{low}	ρ_{up}	Distr.
1	2.0	0.5	4.5	10^3	10^5	Case 1
2	1.8	0.5	4.5	10^3	10^5	Case 1
3	2.0	0.5	4.0	10^3	10^5	Case 1
4	2.0	0.5	3.5	10^3	10^5	Case 1
5	2.0	0.7	4.5	10^3	10^5	Case 1
6	2.0	$-\infty$	4.5	10^2	10^5	Case 1
7	2.0	0.5	4.5	10^2	10^5	Case 1
8	2.0	0.5	4.5	10^3	10^5	Case 2

We generally observe a significant depletion of the globular cluster system. Clusters with masses $M_C \lesssim 10^4 M_\odot$ are destroyed almost everywhere. In the inner part of the Galaxy only about 10 % of the clusters with masses $M_C > 10^5 M_\odot$ survive. Figures 5 and 6 show the final luminosity distribution for two different runs. In the inner part of the Galaxy a peaked luminosity function arises, similar to the observed distribution. The agreement is remarkably good, given our relative simple model. The luminosity function of the outer clusters of the Milky Way is in striking contrast to the inner ones. For the outer clusters one observes no peak. Instead the luminosity function rises slowly to $M_V \sim -8$ and remains fairly constant

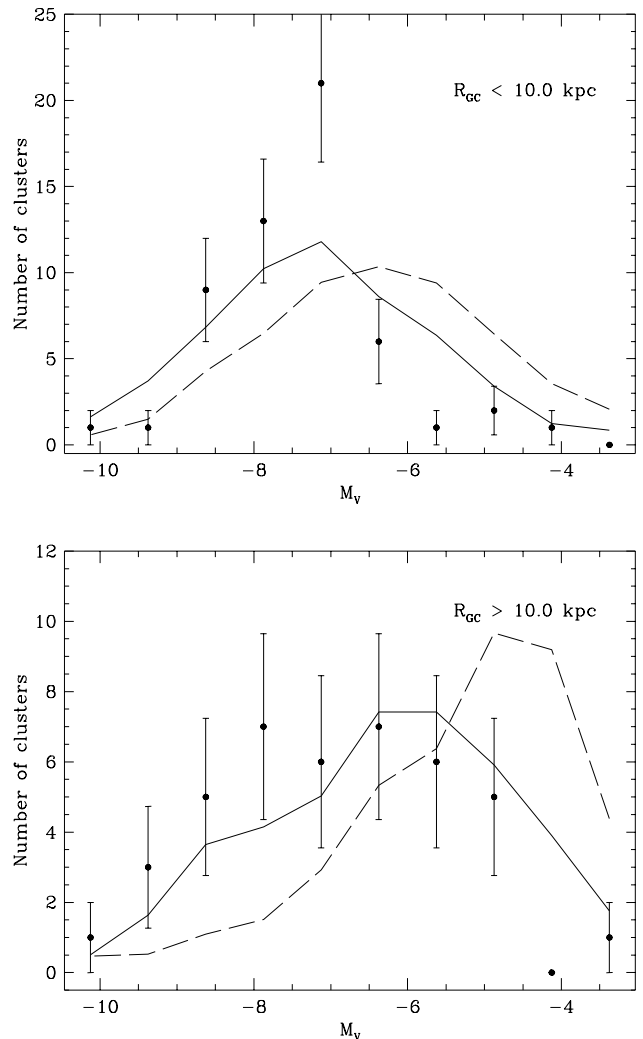


Fig. 5. Plot of the surviving cluster distribution of run 1 (solid lines) against the observations (filled circles). Our distributions are multiplied to contain the same number of clusters as the observations in the two different panels. The dashed line is a simulation with the mass-loss rate halved, but otherwise identical parameters.

afterwards. Here our results do also agree with the observations. Figure 6 shows a run with a shallower initial mass function. The agreement with the observations is also very good, so we cannot constrain the initial power-law index α . But Figs. 5 and 6 show clearly, that it is certainly possible that the Milky Way globular cluster system has started with a power-law mass distribution. This conclusion is similar to that of Okazaki & Tosa (1995), although our method differs significantly from theirs.

Figures 5 and 6 also show the results obtained with the lifetimes of all clusters doubled (dashed lines). In the case of the steeper initial mass function (Fig. 5) it seems to be impossible to match the present-day distribution. In the outer parts a rising luminosity function survives and

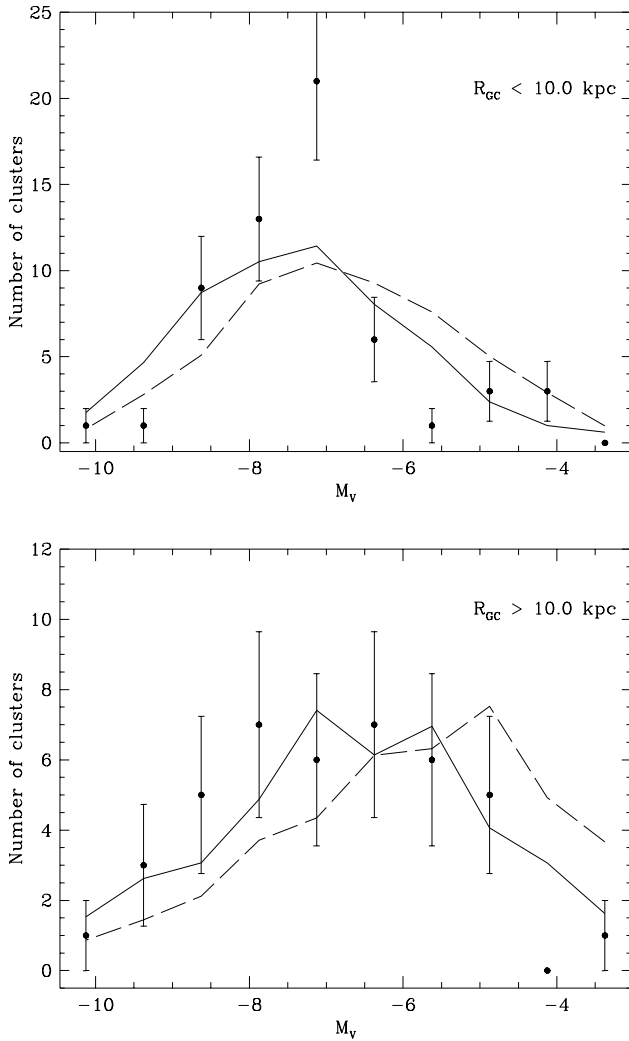


Fig. 6. Same as Fig. 5 but now for run 2.

we generally predict much more low-mass clusters than observed. But the difference is already weaker, if we allow a shallower initial mass function (Fig. 6). One also has to bear in mind that there may be some low-mass clusters near the galactic center, which have been missed by observers due to the strong background of field stars. The same may also be true for clusters far from the galactic center, especially if they have low concentrations. So it seems to be possible to match the present distribution even with all mass-loss rates halved. In the following only the higher mass-loss rates are used.

From the data of Harris (1996) we derive a mean luminosity of $\langle M_V \rangle = -7.15 \pm 0.17$ for the inner halo clusters and $\langle M_V \rangle = -6.89 \pm 0.24$ for the outer. Columns 2 and 3 of table 2 list the mean luminosity of the inner and outer clusters of the surviving distributions. The mean luminosity of the outer clusters is in most cases lower than observed, but in some runs the mean value is within the statistical error (e.g. runs 2 and 5). Our values for the

inner clusters generally agree with the observations, with the exception of run 6. This was a run with all clusters on circular orbits. In this case there are no clusters, which travel from outwards into the inner parts of the Milky Way, hence a great number of low-mass clusters survives due to the weaker tidal field they are exposed to. The luminosity distribution of this run also differs a lot from what is observed.

Table 2. Final parameters of the performed runs

Run	$\langle M_V \rangle$		β		M_{Cl} [M_\odot]	$\frac{M_{Cl}}{M_{Halo}}$
	Inner	Outer	Inner	Outer		
1	-7.1	-6.2	-0.70	-0.14	$6.9 \cdot 10^7$	7.6%
2	-7.3	-6.5	-0.94	+0.09	$6.6 \cdot 10^7$	7.3%
3	-7.0	-6.0	-0.65	+0.04	$5.3 \cdot 10^7$	5.9%
4	-6.8	-5.9	-0.56	+0.03	$4.4 \cdot 10^7$	4.8%
5	-7.0	-6.4	-0.60	+0.10	$9.5 \cdot 10^7$	10.5%
6	-6.6	-5.5	$-\infty$	$-\infty$	$2.0 \cdot 10^7$	2.2%
7	-6.9	-5.9	-1.48	-0.41	$6.1 \cdot 10^7$	6.8%
8	-7.0	-5.6	-1.06	+0.03	$5.4 \cdot 10^7$	6.0%

We next compare the spatial distribution of the surviving clusters with the observations. An initial slope $\gamma = 3.5$ seems to be ruled out since it leads to a final distribution which is too flat compared to the observations (Fig. 7). The present day globular cluster system of the Milky Way follows a density-law $\rho \sim r^{-3.5}$, so the initial distribution must have been steeper because one expects more efficient destruction for the inner clusters due to the stronger tidal field. Indeed we find that $\gamma = 4.0$ or 4.5 is required to match the present distribution. Since the stellar halo has a more flattened distribution, at least in the inner parts, a problem arises. The solution may be that some of the inner clusters are connected to the bulge rather than to the halo. This seems possible since the most metal-poor bulge stars have metallicities comparable to the most metal-rich of the metal-poor clusters (McWilliam & Rich 1994). A varying star cluster to field star formation efficiency may also explain the difference.

Our cluster systems have initially a strongly radially biased velocity distribution. We observe that this bias is reversed to some extent for the final system. This is not surprising, because clusters on radial orbits come close to the galactic center and are preferentially destroyed. Our final velocity distributions become tangentially anisotropic in the inner parts, with a degree which is roughly the same for high-mass ($M_C > 10^5 M_\odot$) and less massive clusters. In the outer parts the velocity anisotropy stays radial, although the degree is weaker. Columns 4 and 5 of Table 2 list the velocity anisotropy parameters of the cluster system. As one can see we generally observe a tangential anisotropy for the inner clusters, even if the system was initially very strongly radially anisotropic (run 5).

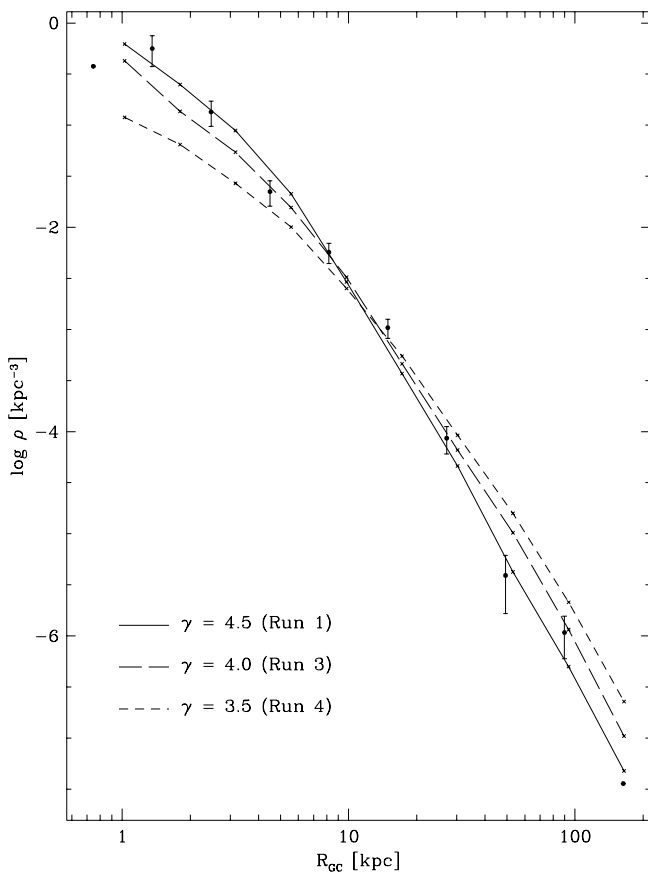


Fig. 7. Run of the density of the final cluster system with galactocentric distance. Three runs are shown with initially different spatial density but otherwise same parameters. Our distributions are shifted vertically to match the number of Milky Way clusters.

We finally calculated the total mass of the cluster system and the fraction of the stellar halo that could have been initially in star clusters (see columns 6 and 7 of Table 2). According to Suntzeff et al. (1990) the mass of the stellar halo between 4 and 25 kpc is $9.0 \cdot 10^8 M_{\odot}$. In order to derive the fraction of stars, which could have been initially in clusters, we calculate the mass of the initial cluster system between 4 and 25 kpc (column 6) and compare it with this value. Typically, we find that about 6% - 10% of the halo mass could initially have been in clusters with masses $M_C > 10^3 M_{\odot}$. Assuming that the number of clusters still rises to $10^2 M_{\odot}$ will typically add only 2% to this value. It seems to be impossible that the complete stellar halo was formed from disrupted globular clusters. On the other hand we have not included in our calculations clusters, which are unbound after formation. Since there is no a priori reason why only stable clusters should form our values are a lower bound and could be higher. Indeed, Schweizer et al. (1996) observed a number of young star clusters in NGC 3921 with extended, often asymmet-

ric shapes, which they interpreted as associations being in the state of dissolution. With this in mind our values are in good agreement to Maoz et al. (1996), who found that between 10 - 25% of the UV-light in merging galaxies comes from compact sources. We note that a similar fraction of the halo stars of the Milky Way could have been formed in star clusters.

Finally the initial number of clusters in the Milky Way should have been of the order of 10^4 . As one would expect, most of these clusters dissolve in the first few Gyr. In the last Gyr of our calculation only between 8 and 10 clusters dissolve. This result is in agreement with Gnedin & Ostriker (1997), who found from Fokker-Planck calculations that between 50% and 90% of the present day clusters will be destroyed within the next 10 Gyr, i.e. 4 to 9 of the halo clusters per Gyr on the average.

The dependence of our results on the initial distribution of half-mass radii is rather weak. Changing the upper limit from 10^3 to $10^2 M_{\odot}/\text{kpc}^3$ (Run 7) for example has only a small effect on the mean luminosity of the inner and outer clusters. Also the total mass that initially could have been in clusters remains roughly the same. The exception is the velocity anisotropy. It becomes more tangential, because it is more important for loosely bound clusters to avoid the galactic center. The same is true for a different distribution of half-mass radii (Run 8). We therefore conclude that our uncertainty concerning the initial distribution over half-mass radius will not affect our results significantly.

4.2. Results for M87

The globular cluster system of M87 is one of the most populous systems yet discovered, with the total number of clusters estimated to be of the order of 13000 (McLaughlin et al. 1994). Due to the fact that the properties of its cluster system are well known and since the different appearance of M87 implies a different dynamical history of its cluster system compared to that of our Galaxy we employed our method to this galaxy.

We compare our results to the observed cluster system from two aspects: the surface density of the clusters as a function of projected radius and the distribution over luminosities at specific radii. For the overall distribution we use the measurements of Grillmair et al. (1986), Harris (1986), McLaughlin et al. (1993) and McLaughlin (1995). The surface densities were corrected for different completeness threshold where necessary. This correction was found to be low. It never exceeded a factor of 1.3 and the measurements show good agreement in the region of overlap, so we expect our final surface brightness profile to be insensitive to variations of the luminosity distribution at different radii. Our corrected densities should be complete to $V = 24$ mag, which corresponds to a cluster mass of $M_C = 1.61 \cdot 10^5 M_{\odot}$ with the adopted distance and mass-to-light ratio. Only clusters more massive than

this were included in the comparison of our results with the observed surface densities.

Recently Whitmore et al. (1995) measured the luminosity distribution of ~ 1000 globular clusters inside $R = 114''$ of the center of M87 with a mean completeness limit of $V = 25.5$ mag. Similar work was done by ES for a 4.57 arcmin² field, 2.5 arcmin away from the center of M87. They found 220 clusters brighter than $V = 26$ mag. These two works were used to check our final luminosity distribution. We first show the results of the calculations with a distance $D = 18$ Mpc. For the M87 cluster system we assume the same distribution as in Run 1 for the Milky Way clusters. We did not try different initial conditions, but from the results of Section 4.1 we expect to obtain similar results. Looking at the space density (Fig. 8a) one can see that the number of massive clusters stays unchanged beyond 80 kpc. Inwards from there the depletion rises steadily. At about 1 kpc the number of clusters is reduced by a factor of 60. This large depletion however is not sufficient to explain the projected density of globular clusters in M87 (Fig. 8b). We can give a crude fit to the profile inside 15 kpc but in that case we predict a density about 5 times lower than the density observed in the outer parts. This underestimation may have two reasons: First, the brightness profile of M87 itself shows deviations from a pure de Vaucouleur law. At $R \gtrsim 40$ kpc for example the galaxy is 1.5 times brighter than our prediction. This will help to reduce the gap but is surely not sufficient. Second, the ratio of stars initially formed in clusters to stars formed in the field may vary with distance from the center: McLaughlin et al. (1993) found 1167 clusters brighter than $V = 24$ mag between 5.6 and 15.0 kpc. According to our calculation the initial number of clusters with masses greater than $M_C = 10^3 M_\odot$ was of the order of 400,000 in this area with a total mass of about $3.2 \cdot 10^9 M_\odot$ in the globular cluster system. The luminous mass of M87 is $1.8 \cdot 10^{11} M_\odot$ in this range, so according to our model only 1.8% of the stars were initially in the cluster system. If M87 is the remnant of several merged spiral galaxies, if globular clusters only arise when galaxies are formed or during merging processes, and if always between 10% and 20% of the stars are built in star clusters in such phases of extraordinary star formation we can draw the following conclusions: (i) In the inner parts only about 20% of the stars were built together with the clusters. Most stars were formed in quiescent phases of star formation, i.e. they are most likely the disks of disrupted spiral galaxies. This is possible, since the mean metallicity of M87 is $[\text{Fe}/\text{H}] = -0.38 \pm 0.89$ (Brodie & Huchra 1991). (ii) In the outer parts the fraction rises significantly and it is possible that all stars were built together with the clusters.

We next compare our results to the luminosity distribution of the clusters at specific radii. Figure 9a compares the surviving clusters inside a circle with projected radius $r_{pr} = 114''$ with the observed clusters of Whitmore et al. (1995). We get a sharply peaked turnover, which fits the

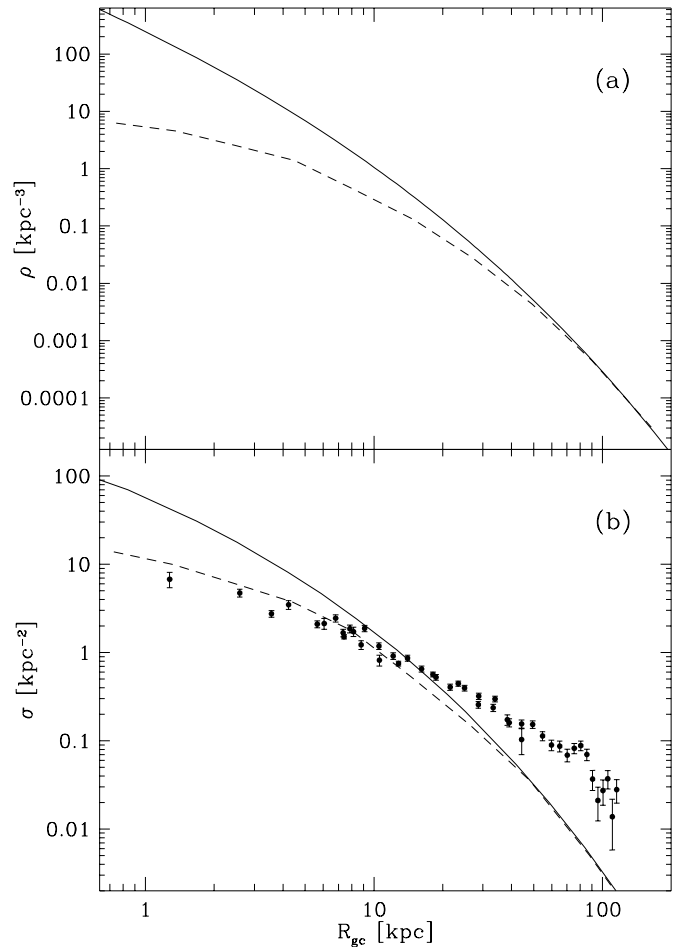


Fig. 8. Run of the density of the final cluster system with distance from the center of M87. The top panel shows the run of the space density. The solid line is the initial de Vaucouleur profile, the dashed line is the final distribution. In the bottom panel we show the projected distributions. The filled circles are the observations. Our final profile (dashed lines) is multiplied to match them inside 15 kpc.

observed luminosity profile very well. This distribution is similar to the inner clusters of the Milky Way and results because low mass clusters have evaporated completely due to the strong tidal field.

If the luminosity function of globular clusters is universal, i.e. the same in all galaxies, globular clusters in a remote galaxy can be used as a distance indicator. To test the universality we now compare the surviving clusters in M87 with the Milky Way clusters. The mean luminosity of the M87 clusters is $M_V = -7.0$, only 0.07 mag fainter than what we found for the globular clusters of run 1 in the inner part of the Milky Way. However changing for example the slope of the power-law of the initial distribution of cluster masses from $\alpha = 2$ to $\alpha = 1.8$ will cause a change of the mean luminosity of $\Delta M_V = -0.3$. If the globular cluster luminosity function is used to measure

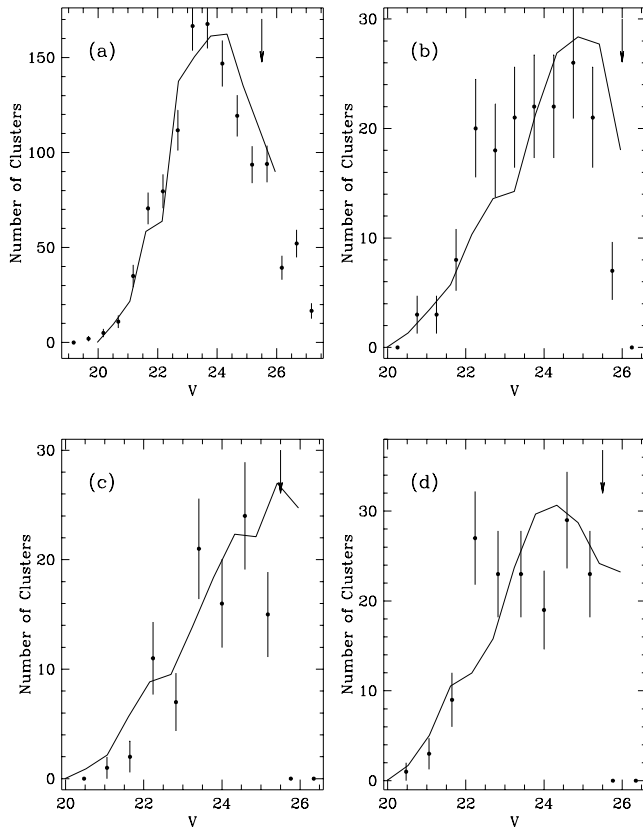


Fig. 9. Comparison of our luminosity distribution (solid lines) with the observations (filled circles) at different radii. a) shows the comparison with Whitmore et al. (1995), b) is the same but now for the ES data. c) shows a run with $T = 10$ Gyr compared to the red clusters of ES, d) shows a run with $T = 16$ Gyr compared to the ES blue clusters. The arrows mark the completeness thresholds in the different panels.

the distance, this corresponds to a change in the derived distance of 15 %, or roughly 3 Mpc with the adopted distance to M87. We observe a similar shift if the mean age of the globular clusters is changed, while the initial velocity anisotropy has only a small effect. We therefore conclude, that the luminosity function of globular cluster systems can only be used to estimate distances, if the initial state of the clusters is exactly the same as in the Milky Way.

One also has to bear in mind, that the luminosity function of the globular clusters varies with distance from the center of their galaxy. This can be seen in Fig. 9b, where we compare our results with the ES data. Their field is roughly 2 times further out from the center than the Whitmore et al. (1995) field. Due to relatively big errorbars no definite answer can be given, but it seems that the peak in the observed luminosity function, if in fact one is present, lies at fainter magnitudes than in Fig. 9a. Our calculations also show a different luminosity function. More low-mass

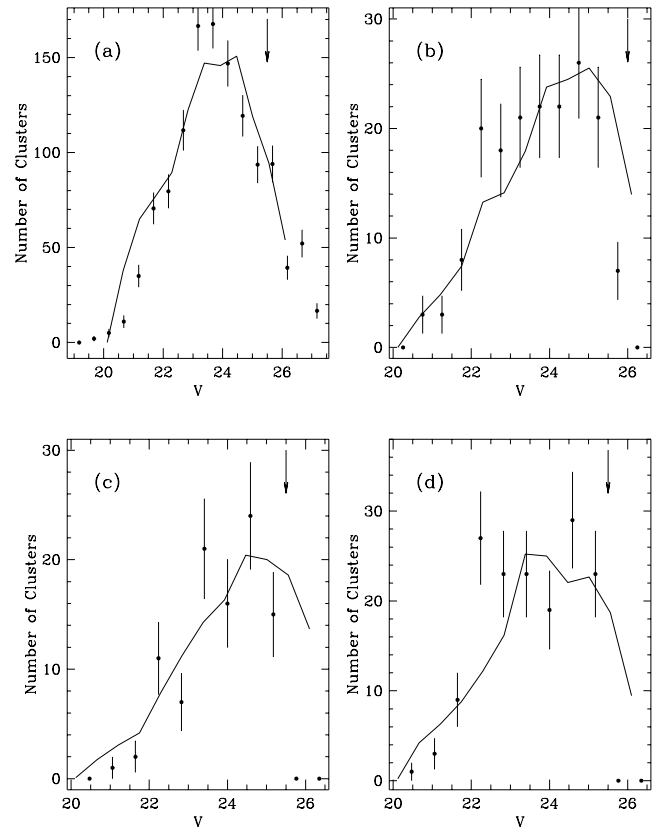


Fig. 10. Same as Fig. 9, but now for a distance $D = 16$ Mpc.

clusters survive due to the weaker tidal field and the peak occurs roughly one mag fainter than for the inner clusters.

ES split their clusters into a blue and a red group. They find that the luminosity distributions between the two groups are different, with the blue clusters being brighter on the average. In order to work out the reason of this difference we made a calculation with a duration of $T = 10$ Gyr and fitted it to the red clusters (Fig. 9c). A second run was made with the same initial distribution, but lasting for 16 Gyr. It was compared with the blue clusters (Fig. 9d). The two runs are a good representation of the observations. The luminosity function of the longer run peaks at a higher magnitude and the clusters are also somewhat brighter. So the different age of the red and blue population may be responsible for the distinct luminosity functions.

We finally present our results for a distance $D = 16$ Mpc. Figure 10 shows our resulting luminosity functions. Both the ES and the Whitmore et al. data are still quite well represented, so we cannot determine the distance to M87. We note that allowing for a different mean age of the globular clusters or a different initial luminosity function will further enlarge the allowed distance range.

5. Summary

We have presented a model for the evolution of globular cluster systems. In our picture globular clusters arise in phases of high star formation activity, for example in the early universe when the galaxies we observe today were formed or during collisions of disk galaxies. Globular clusters always form together with field stars, with roughly one or two tenth of all stars being build in clusters. The luminosity distribution of the clusters at the beginning is a power-law with a slope equal to what is observed for the YLCs in merging galaxies.

Our final distributions are in agreement with the observations. The most striking feature is the development of a peaked profile in the inner parts of the studied galaxies. We find it possible that the initial luminosity distribution was a power law with a power between 1.8 and 2.0. It appears impossible that globular cluster systems start with the same luminosity function that we observe today, because evaporation would have strongly altered the distribution, at least in the inner parts of galaxies.

The different appearance of clusters close to the center of their parent galaxy compared to clusters further out is due to the more efficient dissolution of low mass-clusters through the strong tidal field in the inner part. The peaked luminosity profile in the inner part ($R_{GC} \lesssim 10$ kpc) of the Milky Way and M87 is at least partly caused by the efficient destruction of clusters on highly eccentric orbits. We note that our surviving clusters in the inner parts have in almost all cases a tangential anisotropic velocity distribution.

From the comparison of globular cluster systems in different galaxies we find that the luminosity function is no good distance indicator unless the systems have the same age and initially the same distribution of cluster masses.

Acknowledgements. Many thanks to Roland Wielen for his advise. I also thank Daichiro Sugimoto, Rebecca Elson, Dean McLaughlin and Bradley Whitmore for helpful comments. I especially thank Pavel Kroupa, Rainer Spurzem and Reinhold Bien for a careful reading of this paper and useful discussions.

References

- Aarseth J.S., Heggie D.C., 1993, in *The Globular Cluster-Galaxy connection*, ed. G.H. Smith & J.P. Brodie, ASP Conf. Series 48 (San Francisco: ASP), p. 701
- Armandroff T.E., 1989, *AJ* 97, 375
- Battinelli P., Brandimarti A., Capuzzo-Dolcetta R., 1994, *A&AS* 104, 379
- Beers T.C., Sommer-Larsen J., 1995, *ApJS* 96, 175
- Binney J., Tremaine S., 1987, *Galactic Dynamics*, Princeton Univ. Press, Princeton, p. 425
- Brodie J.P., Huchra J.P., 1991, *ApJ* 379, 157
- Chaboyer B., Demarque P., Sarajedini A., 1996, *ApJ* 459, 558
- de Vaucouleur G., Nieto J.-L., 1978, *ApJ* 220, 449
- de la Fuente Marcos R., 1995, *A&A* 301, 407
- Djorgovski S., Meylan G., 1994, *AJ* 108, 1292
- Elson R.A.W., Santiago B.X., 1996, *MNRAS* 280, 971 (ES)
- Ferrarese L., Freedman W.L., Hill R.J. et al., 1996, *ApJ* 464, 568
- Ford H.C., Harms R.J., Tsvetanov Z.I. et al., 1994, *ApJ* 435, L27
- Giersz M., Heggie D.C., 1994, *MNRAS* 270, 298
- Giersz M., Heggie D.C., 1996, *MNRAS* 279, 1037
- Gnedin O.Y., Ostriker J.P., 1997, *ApJ* 474, 223
- Goodwin S.P., 1997, *MNRAS* 284, 785
- Grillmair C., Pritchett C., van den Bergh S., 1986, *AJ* 91, 1328
- Harris W.E., 1986, *AJ* 91, 822
- Harris W.E., 1991, *ARA&A* 29, 543
- Harris W.E., 1996, available under WWW page: <http://www.physics.mcmaster.ca/Globular.html>
- Hénon M., 1961, *Ann. d'Ap.* 24, 369
- Ho L.C., Filippenko A.V., 1996a, *ApJ* 466, 83
- Ho L.C., Filippenko A.V., 1996b, *ApJ* 472, 600
- King I.R., 1966, *AJ* 71, 64
- Krabbe A., Genzel R., Eckart A. et al., 1995, *ApJ* 447, L95
- Kroupa P., Tout C.A., Gilmore G., 1993, *MNRAS* 262, 545
- Lee H.M., Fahlman G.G., Richer H.B., 1991, *ApJ* 366, 455
- Lee H.M., Goodman J., 1995, *ApJ* 443, 109
- Lyngå G., 1987, *Lund Catalogue of Open Cluster Data*, 5th ed., Stellar Data Centre (Observatoire de Strasbourg, France)
- Maoz D., Barth A.J., Sternberg A. et al., 1996, *AJ* 111, 2248
- McLaughlin D.E., 1995, *AJ* 109, 2034
- McLaughlin D.E., Harris W.E., Hanes D.A., 1993, *ApJ* 409, L45
- McLaughlin D.E., Harris W.E., Hanes D.A., 1994, *ApJ* 422, 486
- McMillan S., Hut P., 1994, *ApJ* 427, 793
- McWilliam A., Rich R.M., 1994, *ApJSS* 91, 749
- Minetti D., 1995, *AJ* 109, 1663
- Morrison H., Flynn C., Freeman K.C., 1990, *AJ* 100, 1191
- Nulsen P.E.J., Böhringer H., 1995, *MNRAS* 274, 1093
- Okazaki T., Tosa M., 1995, *MNRAS* 274, 48
- Ostriker J.P., Spitzer L., Chevalier R.A., 1972, *ApJ* 176, L51
- Preston G.W., Shectman S.A., Beers T.C., 1991, *ApJ* 375, 121
- Pritchett C.J., van den Bergh S., 1994, *AJ* 107, 1730
- Richer H.B., Harris W.E., Fahlman G.G. et al., 1996, *ApJ* 463, 602
- Saha A., Sandage A., Labhardt L. et al., 1996a, *ApJ* 466, 55
- Saha A., Sandage A., Labhardt L. et al., 1996b, *ApJSS* 107, 693
- Sandage A., Saha A., Tammann G.A. et al., 1996, *ApJ* 460, L15
- Sargent W.L.W., Young P.J., Bokserberg A. et al., 1978, *ApJ* 221, 731
- Schweizer F., Miller B.W., Whitmore B.C., Fall S.M., 1996, *AJ* 112, 1839
- Sommer-Larsen J., Flynn C., Christensen P.R., 1994, *MNRAS* 271, 94
- Spitzer L., Hart M.H., 1971, *ApJ* 164, 399
- Suntzeff N.B., Kinman T.D., Kraft R.P., 1990, *ApJ* 367, 528
- Surma P., Seifert W., Bender R., 1990, *A&A* 238, 67
- Travis J., 1994, *Science* 264, 1405
- van der Marel R.P., 1994, *MNRAS* 270, 271
- Weinberg M.D., 1994, *AJ* 108, 1414
- Whitmore B.C., Schweizer F., 1993, *AJ* 106, 1354
- Whitmore B.C., Schweizer F., 1995, *AJ* 109, 960
- Whitmore B.C., Sparks W.B., Lucas R.A., Macchetto F.D., Biretta J.A., 1995, *ApJ* 454, L73
- Wielen R., 1988, in *The Harlow-Shapley Symposium on Globular Cluster Systems in Galaxies*, ed. J.E. Grindlay & A.G.D. Philip, IAU Symposium 126 (Dordrecht, Reidel), p. 393
- Zinn R., 1985, *ApJ* 293, 424

This article was processed by the author using Springer-Verlag L^AT_EX A&A style file L-AA version 3.